4174–4188 *Nucleic Acids Research, 2016, Vol. 44, No. 9* *Published online 15 February 2016*
doi: 10.1093/nar/gkw072

Rad18 confers hematopoietic progenitor cell DNA damage tolerance independently of the Fanconi Anemia pathway *in vivo*

Yang Yang[1,†], Jonathan C. Poe[2,†], Lisong Yang[2], Andrew Fedoriw[3], Siddhi Desai[1], Terry Magnuson[3], Zhiguo Li[4], Yuri Fedoriw[1], Kimi Araki[5], Yanzhe Gao[1], Satoshi Tateishi[6], Stefanie Sarantopoulos[2,*] and Cyrus Vaziri[1,*]

[1]Department of Pathology and Laboratory Medicine, University of North Carolina, Chapel Hill, NC 27599, USA, [2]Department of Medicine, Division of Hematological Malignancies & Cellular Therapy, Duke University, Durham, NC 27710, USA, [3]Department of Genetics, Carolina Center for Genome Sciences, Lineberger Comprehensive Cancer Center, University of North Carolina, Chapel Hill, NC 27599, USA, [4]Department of Biostatistics and Bioinformatics, Duke University, Durham, NC 27710, USA, [5]Institute of Resource Development and Analysis (IRDA) Kumamoto University, Kumamoto 860-0811, Japan and [6]Division of Cell Maintenance, Institute of Molecular Embryology and Genetics (IMEG), Kumamoto University, Kumamoto 860-0811, Japan

Received September 22, 2015; Revised January 11, 2016; Accepted January 31, 2016

ABSTRACT

In cultured cancer cells the E3 ubiquitin ligase Rad18 activates Trans-Lesion Synthesis (TLS) and the Fanconi Anemia (FA) pathway. However, physiological roles of Rad18 in DNA damage tolerance and carcinogenesis are unknown and were investigated here. Primary hematopoietic stem and progenitor cells (HSPC) co-expressed RAD18 and FANCD2 proteins, potentially consistent with a role for Rad18 in FA pathway function during hematopoiesis. However, hematopoietic defects typically associated with *fanc*-deficiency (decreased HSPC numbers, reduced engraftment potential of HSPC, and Mitomycin C (MMC) -sensitive hematopoiesis), were absent in *Rad18*$^{-/-}$ mice. Moreover, primary *Rad18*$^{-/-}$ mouse embryonic fibroblasts (MEF) retained robust Fancd2 mono-ubiquitination following MMC treatment. Therefore, Rad18 is dispensable for FA pathway activation in untransformed cells and the Rad18 and FA pathways are separable in hematopoietic cells. In contrast with responses to crosslinking agents, *Rad18*$^{-/-}$ HSPC were sensitive to *in vivo* treatment with the myelosuppressive agent 7,12 Dimethylbenz[a]anthracene (DMBA). Rad18-deficient fibroblasts aberrantly accumulated DNA damage markers after DMBA treatment. Moreover, *in vivo* DMBA treatment led to increased incidence of B cell malignancy in *Rad18*$^{-/-}$ mice. These results identify novel hematopoietic functions for Rad18 and provide the first demonstration that Rad18 confers DNA damage tolerance and tumor-suppression in a physiological setting.

INTRODUCTION

Cells are frequently subject to DNA damage from environmental, intrinsic and therapeutic sources. Failure to tolerate and accurately repair DNA damage can lead to loss of cell viability or genome instability, an enabling characteristic of cancer cells (1). The E3 ubiquitin ligase RAD18 plays key roles in Trans-Lesion Synthesis (TLS), a DNA damage tolerance mechanism that allows cells to replicate genomes harboring bulky DNA lesions including polycyclic aryl hydrocarbon (PAH) adducts (2). In response to DNA damage, RAD18 redistributes to stalled DNA replication forks (3,4) and mono-ubiquitinates the DNA polymerase processivity factor PCNA (5). DNA damage-tolerant 'Y-family' TLS DNA polymerases possess ubiquitin-binding domains and associate preferentially with mono-ubiquitinated PCNA (6) to promote replicative bypass of DNA lesions and DNA damage tolerance (7). However, TLS polymerases are inherently error-prone when compared to replicative DNA polymerases and can generate mutations. Thus, RAD18 and its effector TLS polymerases can confer viability, but also have the potential to compromise genome stability (7). Indeed *Rad18*-deficient cells are genotoxin-sensitive and hypomutagenic for bypass of various DNA lesions, including PAH (8,9). The RAD18-mediated TLS pathway has been stud-

*To whom correspondence should be addressed. Tel: +1 919 843 9639; Fax: +1 919 966 5046; Email: cyrus_vaziri@med.unc.edu
Correspondence may also be addressed to Stefanie Sarantopoulos. Tel: +1 919 668 4383; Fax: +1 919 668 1091; Email: stefanie.sarantopoulos@duke.edu
†These authors contributed equally to this work as the first authors.

ied extensively in cultured cancer cell lines. However, it is not known if RAD18 contributes DNA damage tolerance *in vivo* or whether mutagenic RAD18-mediated TLS influences carcinogenesis in a physiological setting.

In addition to its role in TLS, RAD18 is implicated as an apical component of the Fanconi Anemia (FA) DNA repair pathway in cultured cancer cells (10–13). FA is a bone marrow failure (BMF) syndrome that is associated with developmental defects, reduced fertility (14,15) and cancer-propensity, in particular Acute Myelogenous Leukemia (16,17). FA can result from congenital defects in any one of the 18 known *FANC* genes whose encoded proteins (termed 'FANCs' A-T) participate in common pathway of DNA replication-coupled inter-strand crosslink (ICL) repair. FA patient cells are hypersensitive to ICL-inducing agents such as Mitomycin C (MMC). When DNA replication forks encounter ICL, a multi-subunit FA 'core complex' mono-ubiquitinates FANCD2 and FANCI (18). Mono-ubiquitinated FANCD2-FANCI is the effector of the FA pathway and directs ICL repair, most likely promoting endolytic processing of crosslinked DNA (19). The FA pathway is also activated in response to many genotoxins that induce replication fork stalling (10), although FANC-deficiencies generally result in more modest sensitivity to DNA lesions other than ICL (20). ICL are complex lesions and ICL repair requires coordination of the FA pathway with three other DNA repair processes including TLS, homologous recombination (HR) and nucleotide excision repair (NER) (17,18).

All hematopoietic lineages are compromised in FA individuals, indicative of hematopoietic stem cell (HSC) dysfunction (16). Indeed, most FA patients have significantly lower numbers of CD34+ cells, a population that is enriched for HSCs and can reconstitute all other hematopoietic lineages upon transplantation. Hematopoietic stem and progenitor cells (HSPC) attrition in FA patients is due to failure to tolerate endogenously-arising DNA lesions (21). Aldehydes, generated via respiratory metabolism, represent a major source of lethal ICL in HSPC from FA individuals (22,23). Unrepaired DNA damage in FA individuals leads to loss of HSPC viability via p53-mediated apoptosis (24). Failure to repair DNA damage appropriately can cause mutations and genome rearrangements that drive cancer. Therefore, the reduced DNA repair capacity of HSC and the ensuing aberrant processing of DNA damage contribute to the hematological malignancy commonly observed in FA.

A relationship between TLS and FA has been suspected for many years for several reasons: (i) TLS is a necessary step in ICL repair. (ii) FA patient-derived and other FANC-defective cells are hypomutable, indicating reduced activity of the TLS pathway when the FA pathway is compromised (25–27). (iii) FANCC is epistatic with the Y-family TLS polymerase REV1 for cisplatin sensitivity in vertebrate cells (27). (iv) The de-ubiquitinating (DUB) enzyme USP1 removes the ubiquitin moiety from mono-ubiquitinated forms of PCNA and FANCD2, thereby coordinating activities of both the TLS and FA pathways (28,29).

Several lines of recent evidence directly implicate RAD18 in FA pathway activation (10–13) and ICL repair (30): in cultured cells, RAD18-deficiency leads to reduced FANCD2 mono-ubiquitination in response to ICL (11), bulky adducts (10) and Topoisomerase I inhibitors (12). In response to bulky DNA lesions and ICL, RAD18-dependent FANCD2 mono-ubiquitination depends upon PCNA mono-ubiquitination and TLS polymerases (10,13). In contrast, RAD18-mediated FANCD2 ubiquitination arising from DNA Topoisomerase I inhibition, is TLS-independent (12). RAD18 also mediates association of the SMC5/6 complex with ubiquitylated proteins in the vicinity of DNA crosslinks, thereby promoting the HR phase of ICL repair in cancer cell lines (30). Combined depletion of RAD18 and FANCD2 does not have additive effects on sensitivity to ICL (11) or Topoisomerase I inhibition (12), indicating an epistatic relationship between RAD18 and the FA pathway.

Published studies showing RAD18-dependent FANCD2 activation in cultured cells raise the interesting possibility that RAD18 is also important for physiological FA pathway functions in hematopoietic genome maintenance, and implicate *RAD18* as a potential *FANC* gene (although no RAD18-deficient FA patients have yet been reported). However, it cannot be assumed that hematopoietic progenitor cells in a physiological setting necessarily rely on the same genome maintenance mechanisms that confer DNA damage tolerance in cultured cell lines. Moreover, cultured cell lines (which are mostly cancer-derived) typically express aberrantly high RAD18 levels when compared with untransformed and primary cells, raising the possibility of neomorphic RAD18 roles in FA pathway activation in (RAD18-overexpressing) cancer cells. Accordingly, the work described here was undertaken to determine the extent to which Rad18 confers hematopoietic genome maintenance *in vivo*. Using Rad18 mutant mice, we have asked whether *Rad18*-deficiency recapitulates the hallmark hematopoietic defects that arise from FA pathway dysfunction and impaired ICL repair. Additionally, we have tested physiological roles of Rad18 in DNA damage tolerance, characterizing the effects of *Rad18*-deficiency on hematopoiesis basally and following exposure to various myelosuppressive genotoxins. Our results define novel roles for Rad18 in hematopoietic DNA damage tolerance and suppression of B cell malignancy. Unexpectedly, we also show that the FA pathway is intact in *Rad18*$^{-/-}$ cells and that *Rad18* mutant mice are phenotypically distinct from *Fanc* mice, indicating that the Rad18 and FA pathways are separable *in vivo*.

MATERIALS AND METHODS

Human CD34+ cell isolation

De-identified, donor leukapheresis discard products and de-identified cord blood samples were obtained with Duke University Medical Center IRB approval. Leukapheresis products were thawed with DNase-containing media before positive selection using Miltenyi CD34+ beads. Freshly acquired Carolinas Cord Blood Bank cells subjected to an EasySep^{TM} Human Cord Blood CD34 Positive Selection Kit. CD34^{+} cell frequency within the CD34-enriched and -depleted fractions was assessed by flow cytometry.

Mice and breeding

Mice were maintained with standard diet in a pathogen-free environment. *Rad18*$^{-/-}$ mice in a C57BL/6J background were described previously (31). 'Knock-in' mice expressing HA-hRAD18 WT and HA-hRAD18-DC2 (mutant lacking amino acids 402–445) from the endogenous *Rad18* promoter were generated as described (32).

Genotoxin administration

7,12-Dimethylbenz[a]anthracene (DMBA, ACROS Organics™) was dissolved in olive oil to [6.66 mg/ml]. Mice were orally-gavaged with DMBA solution (versus olive oil control) to 50 mg/kg. MMC (Sigma) reconstituted in phosphate buffered saline (PBS) was injected i.p. at 1 mg/kg. For H_2O_2 treatments, mice were injected i.v. with freshly-diluted H_2O_2 (in PBS) for final *in vivo* concentration of 200 μM, as described (33).

Bone marrow transplantation

Donor BM cells were harvested from *Rad18*$^{+/+}$ or *Rad18*$^{-/-}$ (CD45.2) and B6.BoyJ (CD45.1 competitor) mice in RPMI 1640 (GIBCO) containing 2% FBS, 10 unit/ml heparin, penicillin and streptomycin. BM cells were centrifuged, washed and re-suspended in serum-free medium. Recipient B6.BoyJ mice were lethally irradiated (1000 cGy) 4 h before injection with 0.2 ml of 1×10^7/ml cells containing a 1:1 mixture of CD45.2 donor and CD45.1 competitor cells. Recipient mice were fed acidified (pH = 2.6), antibiotic-containing water for 4 weeks and acidified antibiotic-free water for the remainder of the experiment. Blood samples were collected from recipient mice 8 and 16 weeks post-transplant. BM cells were harvested 16 weeks post-transplant. CD45.1 and CD45.2 cell subsets were determined by flow cytometry.

Clonogenic analysis of myeloid and B-lymphoid progenitors

BM cells were cultured in Methocult GF M3434 (granulocyte, macrophage–colony-forming units [CFU-GMs]; erythroid–burst-forming units [BFU-Es]; and granulocyte, erythrocyte, macrophage, megakaryocyte–CFUs [CFU-GEMMs]) at 5×10^4 cells/35 mm plate and MethoCult M3630 (CFU–Pre-Bs; Stem Cell Technologies, Vancouver, BC, Canada) at 2×10^5 cells/35 mm dish according to the manufacturer's instructions. Colonies were counted 7 (MethoCult M3630) and 10 days (Methocult GF M3434) after plating.

Cells and culture

Mouse embryonic fibroblasts (MEF) were obtained from day 13 embryos and cultured in Dulbecco's modified Eagle's medium (DMEM) containing 10% fetal bovine serum, streptomycin sulfate (100 μg/ml) and penicillin (100 units/ml). MEF were trypsinized and re-plated at a density of 1:3 after reaching 80% confluence. Swiss 3T3 cells were cultured exactly as described for MEF.

Spermatocyte spreads and immunoflouresence

Spermatocyte spreads were prepared and stained as described elsewhere (34,35). To visualize stained chromosomes, Z-stacks of each channel were taken on a Zeiss AxioImager M2 microscope, using the Axiovision software package (Zeiss). SCP3 and γH2Ax patterns were used to stage spermatocytes, and intensity adjusted for presentation purposes. Primary antibodies (and dilutions) used for immunoflouresence were: SCP3 (Abcam, 1:500), γH2AX (EMD Millipore, 1:1000), rabbit anti-mRad18 (described by Tateishi *et al*. (36), 1:100), rabbit-anti-FANCD2 (Epitomics, 1:50); Secondary antibodies, donkey-anti-rabbit-Alexa647 and donkey-anti-mouse-Alexa568 (Invitrogen) were diluted 1:500. DNA was counterstained with DAPI.

Flow cytometry analysis

For cell cycle analyses, MEF were trypsinized, fixed and propidium iodide (PI)-stained as described (8). PI-stained cells were analyzed on an Accuri C6 flow cytometer (BD, San Jose, CA, USA), and cell cycle profiles generated using FCS express 3 software (De Novo Software, Glendale, CA, USA). For blood and BM (single-cell suspensions prepared from single femurs), RBCs were eliminated using ACK lysis buffer. To detect murine cell surface antigens, viability dye (Zombie Aqua™ Fixable Viability Kit, BioLegend) and anti-CD16/32 to block Fc receptors (TruStain fcX™, BioLegend) were used. Cells were stained using predetermined optimal concentrations of antibodies for 30 min. Antibodies used included: anti-B220 (RA3–6B2), anti-CD43 (1B11), anti-CD4 (GK1.5) and anti-CD127 (IL-7Rα, A7R34), all from BioLegend, Inc. and; anti-Gr-1 (Ly-6G, RB6–85C), anti-CD3 (145–2C11), anti-Sca-1 (D7) and anti-CD117 (c-Kit, 2B8), all from eBioscience, Inc., San Diego, CA, USA. To assess proliferation, intracellular staining for the nuclear proliferation marker Ki-67 (clone SolA15, eBioscience) was performed immediately following cell surface staining according to the manufacturer (using a FoxP3/Transcription Factor Buffer Set, eBioscience). Cells were analyzed on a FACSCanto™ (BD Biosciences) and FlowJo software (version X).

Isolation of LSK, lineage-negative and lineage-committed cells from mouse bone marrow

Single-cell suspensions of total bone marrow cells were prepared from the bilateral femurs of C57Bl/6 mice. Lineage-committed cells were then removed with magnetic beads using a mouse Lineage Cell Depletion Kit (Miltenyi Biotec, Inc.). Lineage-negative cells were subsequently stained with antibodies against Sca-1 (D7) and CD117 (c-Kit, 2B8) to identify the LSK population, with 7-AAD added to exclude dead cells. Viable LSK cells and lineage-negative cells depleted of the LSK subset were then each isolated using a MoFlo™ XDP cell sorter (Beckman Coulter, Inc). The LSK subset was verified to at least 94% pure as determined by post-sort flow cytometry analysis. Cell extracts of LSK cells, LSK-depleted lineage-negative cells and lineage-committed cells depleted of RBCs (using ACK lysis buffer) were prepared and analyzed by SDS–PAGE with immunoblotting as described below.

SDS-PAGE and immunoblotting

Cell extracts were prepared and analyzed by SDS-PAGE with immunoblotting as described previously (8). Primary antibodies were: p-ATM S1981 (SC-47739), β-actin (SC-130656), mouse monoclonal PCNA clone PC10 (SC-56), GAPDH (SC-32233, Santa Cruz Biotechnology Inc.); Rad18 (A301–340A, Bethyl Laboratories Inc.; ATM (GTX70104, Gene Tex); mouse monoclonal γH2AX S139 (05–636, EMD Millipore); and FANCD2 (2986–1, Epitomics Inc.).

Statistics

Group comparisons of flow cytometry data and cell survival results were analyzed by Student's *t*-test. Tumor subtype frequency comparison was analyzed using Chi square test. The frequency of Fancd2 distribution to asynaptic chromosomes in mice from different genotypes was analyzed by Chi square test.

RESULTS

Expression of Rad18 and Fancd2 in hematopoietic progenitors

We examined the relative expression levels of Rad18 and Fancd2 proteins in different subsets of hematopoietic progenitor cells from wild-type mice. As expected, Fancd2 was expressed highly in isolated (Lin-)/Sca-1+/c-kit+ (LSK) cells, a population containing the most primitive hematopoietic stem cells that possess self-renewal capacity and can give rise to all other lineages present in the BM and circulating blood. Fancd2 was also expressed in lineage-negative (Lin-) cells that do not yet express markers of more mature lineage-committed blood cells. However, in lineage-committed (Lin+) cells Fancd2 was expressed at only 5% of the levels present in LSK and Lin- cells (Figure 1A, lane 3 of Fancd2 blot). The expression profile of Fancd2 in different progenitor subsets is consistent with the established roles of the FA pathway in genome maintenance of primitive hematopoietic progenitors.

Similar to FANCD2, Rad18 was expressed in LSK cells, but was expressed at greatly reduced levels (∼3%) in the Lin− cells and was undetectable by immunoblotting in Lin+ cells (Figure 1A, lanes 2 and 3 of Rad18 blot). For the purpose of comparison, we examined expression of Chk1, an S-phase checkpoint kinase that is typically activated coincident with Rad18 and the FA pathway in response to replication fork stalling. Similar to FANCD2, Chk1 was expressed at high levels in LSK and Lin− populations, but not in Lin+ cells. Therefore, Rad18 and Fancd2 are specifically co-expressed in LSK cells, but not in the Lin− population. These expression profiles are potentially consistent with a role for Rad18 in FA pathway activation in some mouse hematopoietic progenitor subsets.

For the purpose of comparison with mouse LSK cells, we also examined relative expression of Rad18 and FANCD2 in human HSC. In humans, CD34+ hematopoietic progenitors are enriched in HSC and critically require the FA pathway for their normal functions *in vivo* (24). Using leukapheresis samples from G-CSF-treated healthy human donors we isolated CD34+ cells and analyzed Rad18 and FANCD2 levels by immunoblot. Purity of the CD34+ cells was >90% (Figure 1B). Both Rad18 and FANCD2 were highly expressed in CD34+ cells relative to the more differentiated CD34− cells. Similar to leukapheresis-derived samples, we detected expression of Rad18 (and FANCD2) only in CD34+ cells from fresh human umbilical cord blood (Figure 1C). Moreover, expression of Rad18 and FANCD2 was insensitive to *in vitro* culture with G-CSF. The high-level co-expression of Rad18 in CD34+ cells is consistent with a role for Rad18 in primitive hematopoietic stem cell function and hematopoiesis in mice and humans.

Rad18-FA signaling and ICL-tolerance in Rad18$^{-/-}$ cells

Since cells from FA patients are hypersensitive to ICL-inducing agents such as MMC, we tested the role of Rad18 in FA pathway activation and ICL tolerance in primary mouse cells. FA cells undergo an aberrant and persistent G2 arrest in response to MMC treatment, owing to inappropriate processing of ICL to DNA breaks (37,38). As shown in Figure 1D, a 48 h treatment with 15 nM MMC led to a 2-fold increase in the G2/M population of primary *Rad18*$^{+/+}$ MEF but increased the G2/M population of *Rad18*$^{-/-}$ cells by 3.6-fold (Figure 1D). The aberrant MMC-induced G2/M arrest of *Rad18*-null cells was also evident when we used independent isogenic cultures of *Rad18*$^{+/+}$ and *Rad18*$^{-/-}$ littermate MEF derived from a different pregnant female (Supplementary Figure S1). When comparing the two independent sets of isogenic MEF, in *Rad18*$^{+/+}$ cells 15 nM MMC induced a 2.05 ± 0.05-fold increase in the G2/M population, whereas in *Rad18*$^{-/-}$ MEF, 15 nM MMC induced a 3.9 ± 0.3-fold increase in G2/M content, a difference between genotypes that is statistically significant by conventional criteria ($P = 0.026$).

The aberrant G2/M arrest of *Rad18*$^{-/-}$ MEF recapitulates a hallmark ICL-tolerance defect of FA cells. Surprisingly, however, the MMC-induced G2 arrest of *Rad18*$^{-/-}$ MEF was associated with a 2.0-fold increase in ubiquitination and chromatin-association of Fancd2 that was identical to the fold-increase in Fancd2 chromatin binding in WT cells (Figure 1E). Therefore, Rad18 is dispensable for ICL-induced FA pathway activation in primary cells. Interestingly, basal levels of Fancd2 on chromatin were 2.4-fold higher in *Rad18*$^{-/-}$ cells when compared with WT MEF. The increased chromatin binding of Fancd2 in *Rad18*$^{-/-}$ cells likely reflects compensatory activation of the FA pathway to enable tolerance of DNA replication stress tolerance when TLS is absent. *Rad18*$^{-/-}$ MEF were MMC-sensitive when compared with *Rad18*$^{+/+}$ MEF, as shown by clonogenic survival assays (Figure 1F and Supplementary Figure S1).

The MMC-sensitivities of *Rad18*$^{-/-}$ MEF fully recapitulate the expected MMC-tolerance defects of *Fanca*$^{-/-}$ fibroblasts (Supplementary Figure S2) as revealed under identical experimental conditions. As expected, *Fanca*$^{-/-}$ cells lacked the slowly-migrating mono-ubiquitinated species of Fancd2, although Fancd2 mono-ubiquitination is intact in *Rad18*$^{-/-}$ MEF (Figure 1E). We conclude that Rad18 is not an obligate upstream component of the FA pathway and contributes to MMC tolerance in-

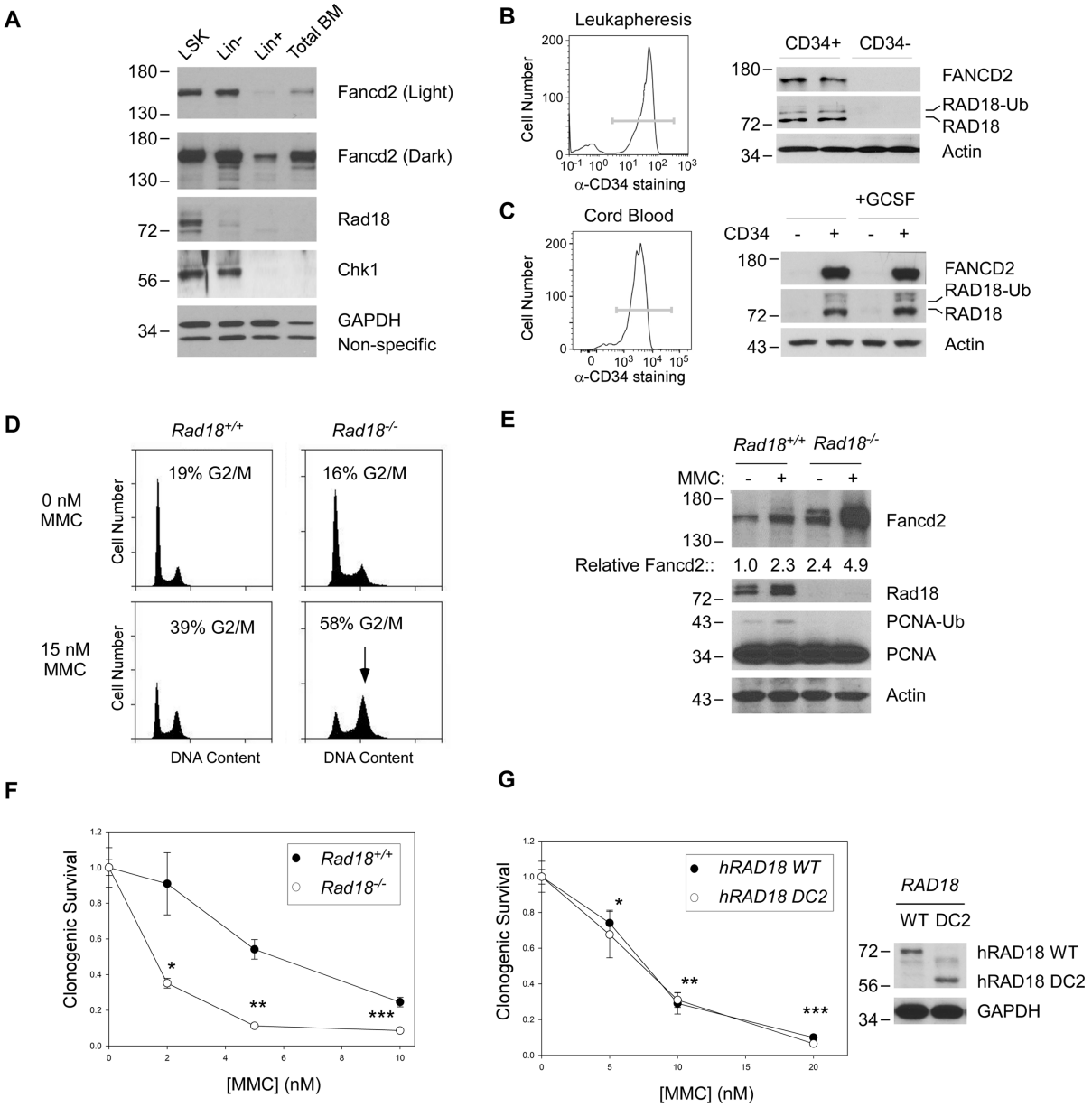

Figure 1. RAD18 is expressed in HSPC and confers ICL-resistance in primary MEF. (**A**) LSK cells, Lin− cells and Lin+ populations were isolated from total BM cells of *Rad18*$^{+/+}$ mice as described under Materials and Methods. Protein extracts from the resulting populations were resolved by SDS-PAGE and analyzed by immunoblotting with antibodies against Fancd2, Rad18, Chk1 and GAPDH. (**B**) CD34+ and CD34− cells were isolated from GCSF-provoked human leukapheresis product. Purity of the CD34+ population was verified by anti-CD34-staining and flow cytometry (left panel). Extracts from the purified cells were resolved by SDS-PAGE and analyzed by immunoblotting with antibodies against Rad18, Fancd2 and β-Actin (loading control). (**C**) CD34+ and CD34− cells were isolated from human umbilical cord blood. Purity of the CD34+ population was verified by anti-CD34-staining and flow cytometry (left panel). CD34+ and CD34− cells were resuspended in RPMI medium and cultured for 18 h in the presence or absence of G-CSF (Neupogen, 500 ng/ml). The resulting cells were washed with PBS and lysed. Cell extracts were resolved by SDS-PAGE and analyzed by immunoblotting with antibodies against Rad18, Fancd2 and β-Actin (loading control). (**D**) Replicate cultures of exponentially-growing *Rad18*$^{+/+}$ and *Rad18*$^{-/-}$ MEF were incubated for 48 hr with MMC (30 nM) or were left untreated for controls. Nuclei from the resulting cells were stained with PI and DNA contents of all samples were analyzed by flow cytometry. (**E**) Replicate cultures of exponentially-growing *Rad18*$^{+/+}$ and *Rad18*$^{-/-}$ MEF were incubated for 2 h with MMC (60 nM) or were left untreated for controls. Chromatin fractions obtained from the resulting cultures were resolved by SDS-PAGE and analyzed by immunoblotting with antibodies against Fancd2, Rad18, PCNA and Actin. (**F**) Replicate cultures of exponentially-growing *Rad18*$^{+/+}$ and *Rad18*$^{-/-}$ MEF were incubated with various doses of MMC for 2 days and analyzed for clonogenic survival. On the survival curves, each data point represents the mean of three replicate determinations and error bars represent the range. For each dose of MMC, we performed unpaired Student's *t*-test between between groups. For cells that received 2, 5 or 10 nM MMC, the *P*-values were 0.0055, 0.0002 and 0.0006, respectively, indicating significant differences between MMC-tolerance of *Rad18*$^{+/+}$ and *Rad18*$^{-/-}$ cells. (**G**) Replicate cultures of exponentially-growing MEF from *hRAD18 (WT)* and *hRAD18 DC2* knock-in mice were incubated with various doses of MMC for 2 days and analyzed for clonogenic survival (left panel). On the survival curves, each data point represents the mean of three replicate determinations, and error bars represent the range. Statistical significance was determined as described in (F) above. For cells that received 5, 10 or 20 nM MMC, the *P*-values were 0.49, 0.67 and 0.6, respectively, indicating no significant differences between MMC-tolerance of *hRAD18 (WT)* and *hRAD18 DC2* MEF. Whole cell extracts from *hRAD18 (WT)* and *hRAD18 DC2* MEF were resolved by SDS-PAGE and analyzed by immunoblotting with anti-Rad18 antibodies to verify equivalent expression of the wild-type and mutant hRAD18 proteins (right panel).

dependently of its previously described proximal role in mediating Fancd2 ubiquitination in cancer cells (10,30). To determine whether Rad18 and the FA pathway function in a common pathway of ICL-tolerance in primary mouse cells (as previously reported using cancer cell lines) we determined the effects of individual and combined Rad18 and *Fanca*-deficiencies on MMC-sensitivity. Using Rad18-directed siRNA we achieved >95% depletion of Rad18 in both $Fanca^{+/+}$ and $Fanca^{-/-}$ cells (Supplementary Figure S2B). Rad18-depletion had no effect on Fancd2 levels or monoubiquitination (as expected), and did not further sensitize the *Fanca* mutant MEF to MMC. Because partial Rad18-depletion did not sensitize *Fanca*-mutant MEF to MMC, Rad18 probably functions downstream of the FA pathway. However, Rad18-knockdown did not sensitize $Fanca^{+/+}$ MEF to MMC, whereas $Rad18^{-/-}$ MEF were MMC-sensitive (see Figure 1F and Supplementary Figure S1). We conclude therefore that the low residual levels of Rad18 (<5%) present in siRad18-transfected MEF are sufficient to support normal MMC-tolerance.

In human cancer cells, Rad18 facilitates association of the SMC5/6 complex with ubiquitylated proteins in the vicinity of DNA crosslinks to promote DNA repair (30). To determine the contribution of Rad18-Smc5/6 interactions to MMC-tolerance, we prepared MEF from 'knock-in' mice expressing physiological levels of wild-type hRAD18 or the hRAD18 'DC2' mutant (which lacks the SMC5/6-interacting domain) from the endogenous *Rad18* promoter. As shown in Figure 1F, *hRAD18* (WT) and *hRAD18 DC2* MEF expressed similar levels of RAD18 protein and showed normal MMC tolerance. As expected, ubiquitination of Fancd2 was not compromised in *hRAD18 DC2* MEF when compared with *hRAD18* WT cells (Supplementary Figure S3). Taken together, results of Figure 1C–F show that Rad18 is dispensable for FA pathway activation in response to MMC, and confers ICL-tolerance independently of its association with Smc5/6 in primary MEF.

Rad18-deficiency does not recapitulate basal hematopoietic defects of *Fanc* mutant mice

The defective ICL tolerance of *Fanc* mutant mice typically leads to decreased HSC numbers (15,39,40). We quantified hematopoietic cells in peripheral blood and bone marrow from WT and $Rad18^{-/-}$ mice. As shown in Figure 2A and B, there was no statistically-significant difference in the numbers of total cells, Lin−, LSK or CLP populations in the BM when comparing $Rad18^{+/+}$ and $Rad18^{-/-}$ mice. In the peripheral blood, there were modest but significant ($P < 0.05$) increases in T and B cells in $Rad18^{-/-}$ mice (1.5-fold for T cells, 1.6-fold for B cells), but these changes were independent of progenitor cell numbers in the BM. Taken together, these results show that there is no basal hematopoietic defect in Rad18-deficient mice.

Fanc-deficient HSPC have reduced capacity for complementation of hematopoiesis in irradiated recipient animals which lack a functional immune system (39,41–43). Therefore, bone marrow transplant (BMT) experiments were performed to compare the engraftment potential of donor $Rad18^{+/+}$ and $Rad18^{-/-}$ HSC. BM cells from $Rad18^{+/+}$ or $Rad18^{-/-}$ mice (expressing CD45.2) were mixed with CD45.1competitor BM cells and transplanted into lethally-irradiated hosts (see Figure 2C). After 8 weeks, donor chimerism was determined by flow cytometric staining of nucleated peripheral blood cells with anti-Cd45.1 and anti-CD45.2 in the recipient mice (41). After 16 weeks, donor chimerism was determined for both nucleated peripheral blood cells and BM progenitors. As shown in Figure 2D, $Rad18^{-/-}$ donor BM efficiently reconstituted all hematopoietic cell subsets analyzed in lethally-irradiated recipient mice. No significant differences in reconstitution efficiency were observed between WT and $Rad18^{-/-}$ donor BM.

Next we asked whether FA-like phenotypes of $Rad18^{-/-}$ mice could be revealed by genotoxin challenge. In the C57BL6 background a single dose of 1 mg/kg MMC kills $Fancc^{-/-}$ (but not WT) mice in within 10 days (40). In contrast with *Fancc* mutants, $Rad18^{-/-}$ (and $Rad18^{+/+}$) mice tolerated 1 mg/kg MMC and showed no adverse health effects (body weight, grooming, posture and activity) for at least 3 weeks (not shown). Therefore, $Rad18^{-/-}$ mice do not phenocopy the sensitivity of *Fanc* mice to 1 mg/kg of MMC. In other experiments we treated $Rad18^{+/+}$ and $Rad18^{-/-}$ mice with a range of higher MMC concentrations including 1, 2, 4 and 8 mg/kg. An MMC concentration of 8 mg/kg killed both $Rad18^{+/+}$ and $Rad18^{-/-}$ mice after 9 days. There was no MMC concentration or length of treatment that selectively killed $Rad18^{-/-}$ mice but not WT animals, consistent with our overall conclusion that Rad18 is not a major contributor to the FA pathway and ICL resistance *in vivo*.

We also determined the effects of MMC on hematopoietic cells in the peripheral blood and bone marrow including the repopulating lineage negative LSK and Lin-/Sca-1+/c-kit-IL-7Rα+ common lymphoid progenitor (CLP) populations. Remarkably, $Rad18^{-/-}$ mice had no detectable impairment in hematopoietic cell development or in peripheral immune cell subsets relative to WT control mice (Figure 3A). Hematopoietic cells in $Fanca^{-/-}$ mice are sensitive to H_2O_2-induced genotoxicity (33). However, as shown in Figure 3B, Rad18-deficiency did not lead to defective H_2O_2 tolerance in LSK cells or other lineages. We conclude that while Rad18 may sometimes contribute to FA pathway in cultured cells, Rad18-deficiency does not compromise normal hematopoiesis or recapitulate hallmark hematopoietic genotoxin-sensitivities of *Fanc*-deficient mice.

Rad18 confers hematopoietic PAH tolerance

Next, we tested whether Rad18 contributes to maintenance of normal hematopoietic function following *in vivo* exposure to other classes of genotoxins. DMBA, a PAH, targets hematopoietic progenitors, leading to anemia in the short term (44–47) and hematological malignancy in the long term (48–50). The genome maintenance pathways that prevent hematopoietic dysfunction following PAH exposure have not been investigated.

As shown in Figure 4A, Rad18-depleted 3T3 cells aberrantly accumulated the DSB markers ATM (pS1981) and γH2AX following DMBA treatment, showing that Rad18 confers DMBA-tolerance, at least in cultured cells. To test a potential role for Rad18 in protecting hematopoietic pro-

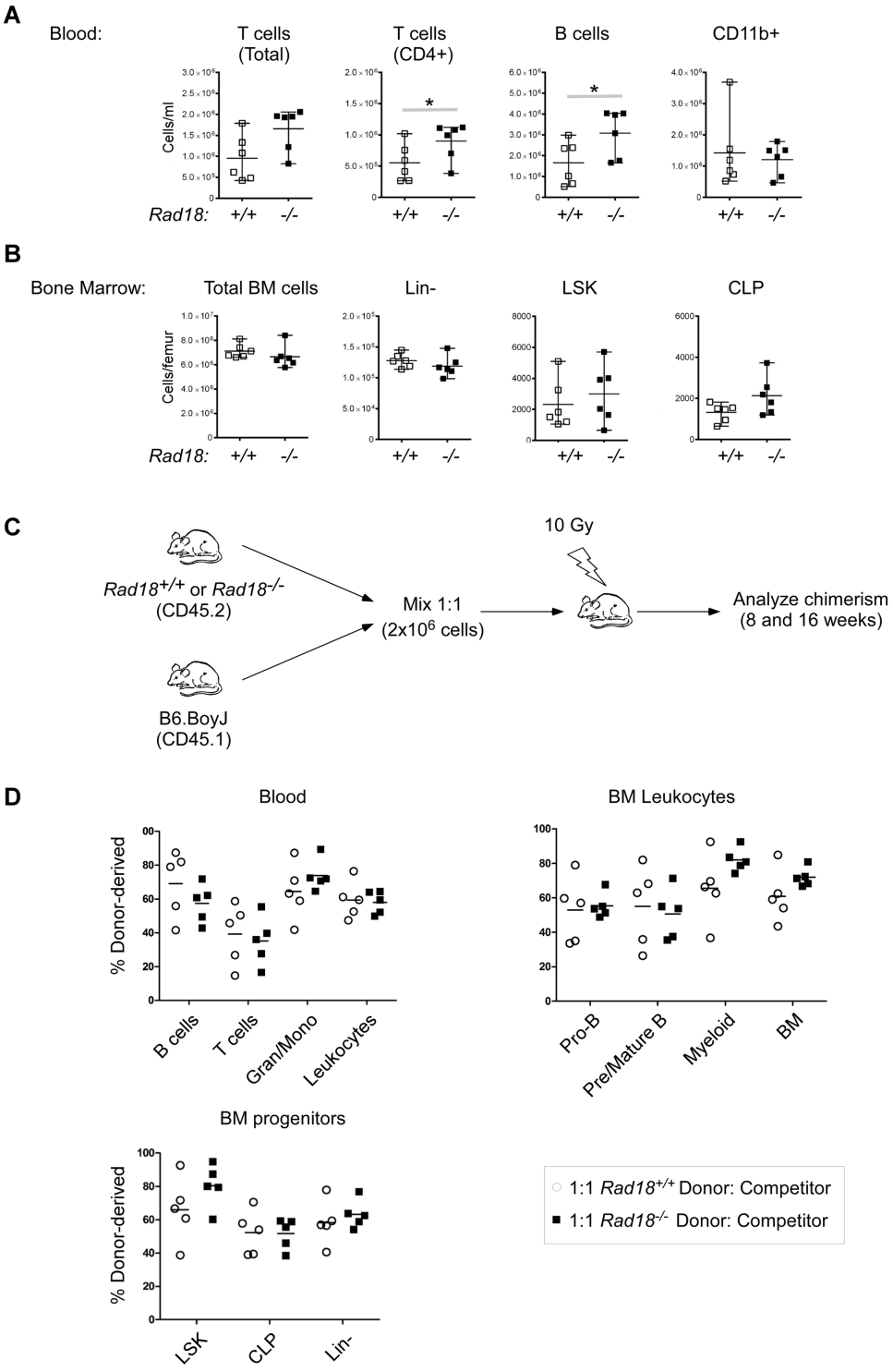

Figure 2. Rad18 deficiency does not impair hematopoiesis in otherwise normal mice. (**A** and **B**) Blood and bone marrow cells isolated from un-manipulated *Rad18*$^{-/-}$ mice and their WT littermates were stained for cell surface markers and assessed for populations of interest by flow cytometry. Each data point represents the cell number results from an individual mouse, with the mean indicated for each group (see Supplementary Figure S1 for bone marrow progenitor cell gating strategy). (**C**) Experimental scheme used to determine effects of Rad18-deficiency on bone marrow engraftment following HSCT. Lethally-irradiated WT B6.SJL recipient mice (CD45.1 allele) were reconstituted with donor bone marrow from *Rad18*$^{-/-}$ mice or their WT littermates (each harboring the CD45.2 allele). Prior to transfer, donor bone marrow from each mouse was mixed with competitor bone marrow from normal B6.SJL mice at a 1:1 ratio. 16 weeks following transfer, blood and bone marrow of recipient mice were assessed for the frequency of donor CD45.2 cells in various cell subsets by flow cytometry. (**D**) Blood and bone marrow were obtained from HSCT recipient mice and assessed for the frequency of donor CD45.2 cells in various cell subsets by flow cytometry, defined by the percentage of total CD45.1+ and CD45.2+ donor cells (see Supplementary Figures S4 and S5 for bone marrow progenitor cell gating strategy). Statistical analysis was performed using an unpaired, two-tailed Student's *t*-test. Mean values significantly different between genotypes are indicated (*$P < 0.05$).

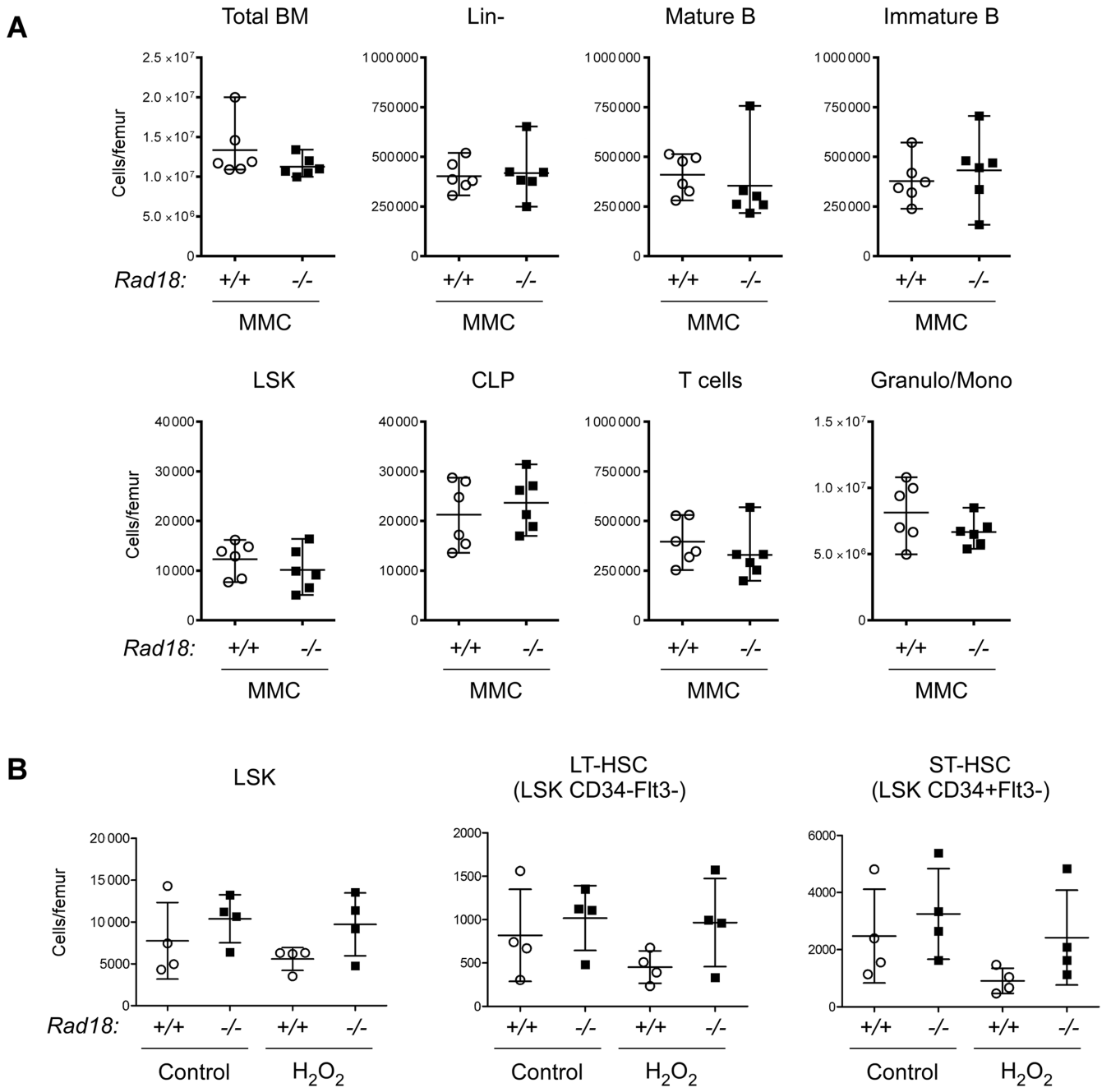

Figure 3. Rad18-deficiency does not recapitulate hematopoietic genotoxin-sensitivities of *Fanc*-deficient mice. *Rad18*$^{-/-}$ mice or their WT littermates were treated with a single dose of MMC (**A**) or H_2O_2 (**B**) as described in 'Materials and Methods'. Five days following MMC treatment and 24 h following H2O2 treatment, mice were euthanized and their bone marrows assessed for cell populations of interest by flow cytometry. Statistical analysis was performed using an unpaired, two-tailed Student's *t*-test. No cell subset comparisons between genotypes or different treatment groups of the same genotype reached statistical significance.

genitors from PAH-induced DNA damage *in vivo* we used an established experimental regimen (Figure 4B) in which short-term DMBA treatment induces myelosuppression and chronic repeat DMBA treatments lead to hematopoietic malignancy (44,45,47,51). As shown in Figure 4C, the numbers of LSK cells in the BM of *Rad18*$^{-/-}$ mice were reduced to 25% ($P < 0.01$) of the population present in WT mice after a single DMBA challenge. The LSK population was specifically sensitive to depletion by a single DMBA dose, while other cell populations (including B cells, T cells, CLP and Lin- cells) were largely unaffected (Figure 4C). Therefore, the repopulating LSK subset is likely to be the most sensitive to short-term DNA damage, with Rad18 playing a clear role in LSK maintenance under these conditions.

We asked whether the Rad18-Smc5/6 interactions that contribute to MMC-tolerance in cancer cells (30) are involved in DMBA-tolerance *in vivo*. Therefore, we com-

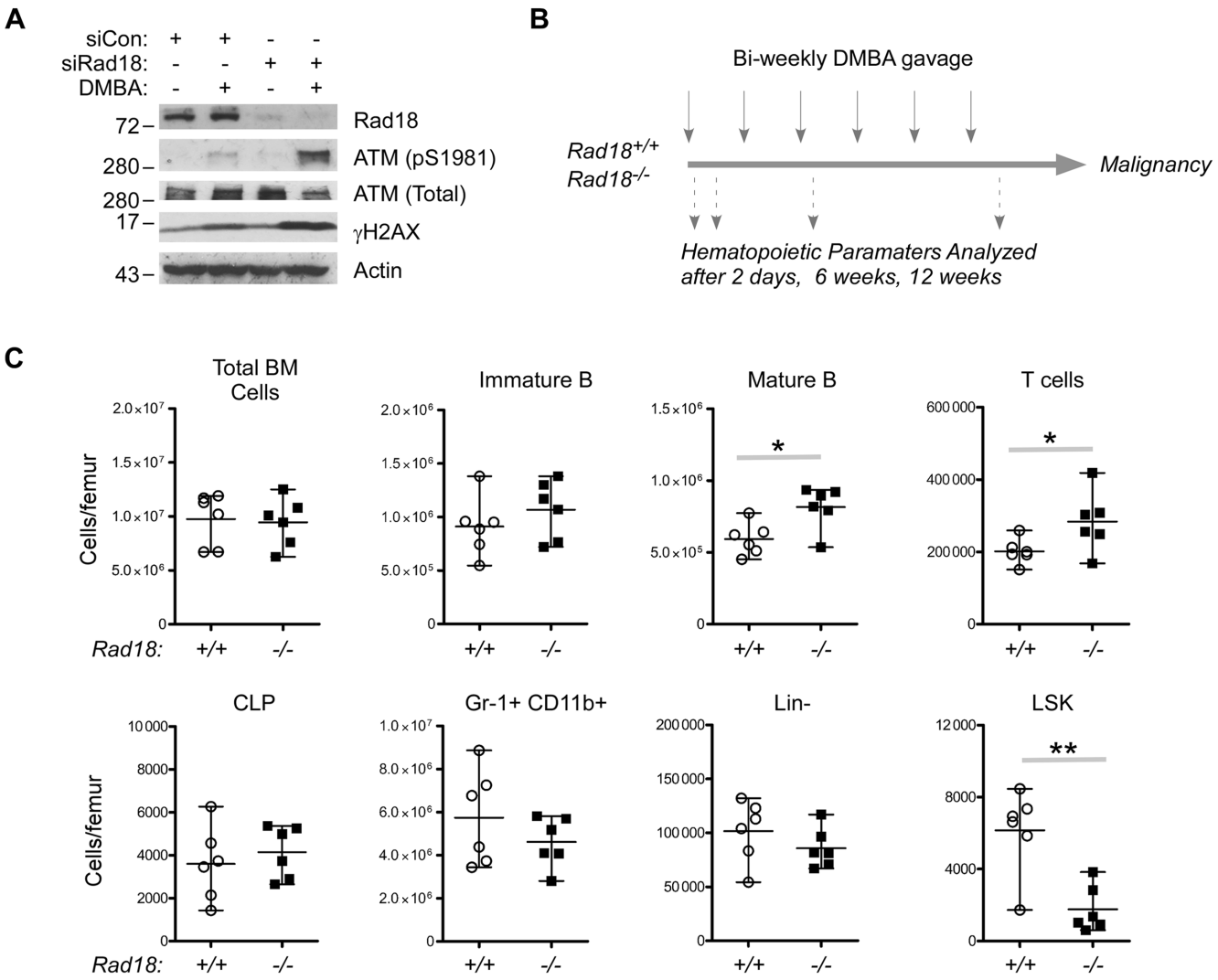

Figure 4. DMBA-sensitivity of Rad18-depleted Swiss 3T3 fibroblasts and hematopoietic progenitors. (**A**) Replicate cultures of Swiss 3T3 cells were transfected with siRNA against Rad18 (siRad18) or with non-targeting control oligonucleotides (siCon). The resulting cultures were treated with 1 μM DMBA for 24 h. Chromatin extracts were prepared from the resulting cells and subject to SDS-PAGE and immunoblotting with the indicated antibodies. (**B**) Summary of DMBA treatment regimen used in this study to determine DNA damage-sensitivities and carcinogenesis in *Rad18*$^{+/+}$ and *Rad18*$^{-/-}$ mice. (**C**) *Rad18*$^{+/+}$ and *Rad18*$^{-/-}$ mice were treated with a single dose of DMBA (50 mg/kg). Forty eight hours later bone marrow cells from the DMBA-treated mice were stained with antibodies against appropriate cell surface markers and assessed for various hematopoietic cell subsets using flow cytometry. Statistical analysis was performed using an unpaired, two-tailed Student's *t*-test. Mean values significantly different between genotypes are indicated (*$P <$ 0.05; **$P < 0.01$).

pared the MMC-sensitivity of hematopoietic progenitors in knock-in mice expressing WT and DC2 (SMC5/6-interaction-deficient) *hRAD18* alleles. As shown in Supplementary Figure S6, there were no significant differences in numbers of total BM cells, LSK cells or Lin− cells basally or after DMBA-treatment when comparing *hRAD18 (WT)* and *hRAD18 DC2* mice. We conclude that the Rad18-Smc5/6 interaction that confers MMC-tolerance in cancer cells (30) does not contribute significantly to maintenance of hematopoietic progenitors basally or after DMBA treatment *in vivo*.

Based on the sensitivity of LSK cells to a single dose of DMBA, we hypothesized that repeat DMBA challenge would prematurely exhaust HSPC pools in *Rad18*-deficient animals. Therefore, *Rad18*$^{+/+}$ and *Rad18*$^{-/-}$ mice were administered three bi-weekly doses of DMBA or were left untreated for controls. The *in vivo* engraftment potential of HSPC from the DMBA-treated animals was determined using BMT (Figure 5A). Sixteen weeks post-transplant, analysis of donor chimerism of recipient mice showed specific reductions in numerous cell populations derived from DMBA-treated *Rad18*$^{-/-}$ donor mice (CD45.2+) in BM (Figure 5B) and blood (Figure 5C). For example in the BM, numbers of *Rad18*$^{+/+}$ progenitor-derived mature B-cells, T-cells and LSK cells were modestly affected (27% decrease for mature B cells, $P < 0.05$; 30% decrease for T-cells, $P <$ 0.05) or unaffected (LSK cells, no significant difference) by prior DMBA treatment of the donor mice. However, num-

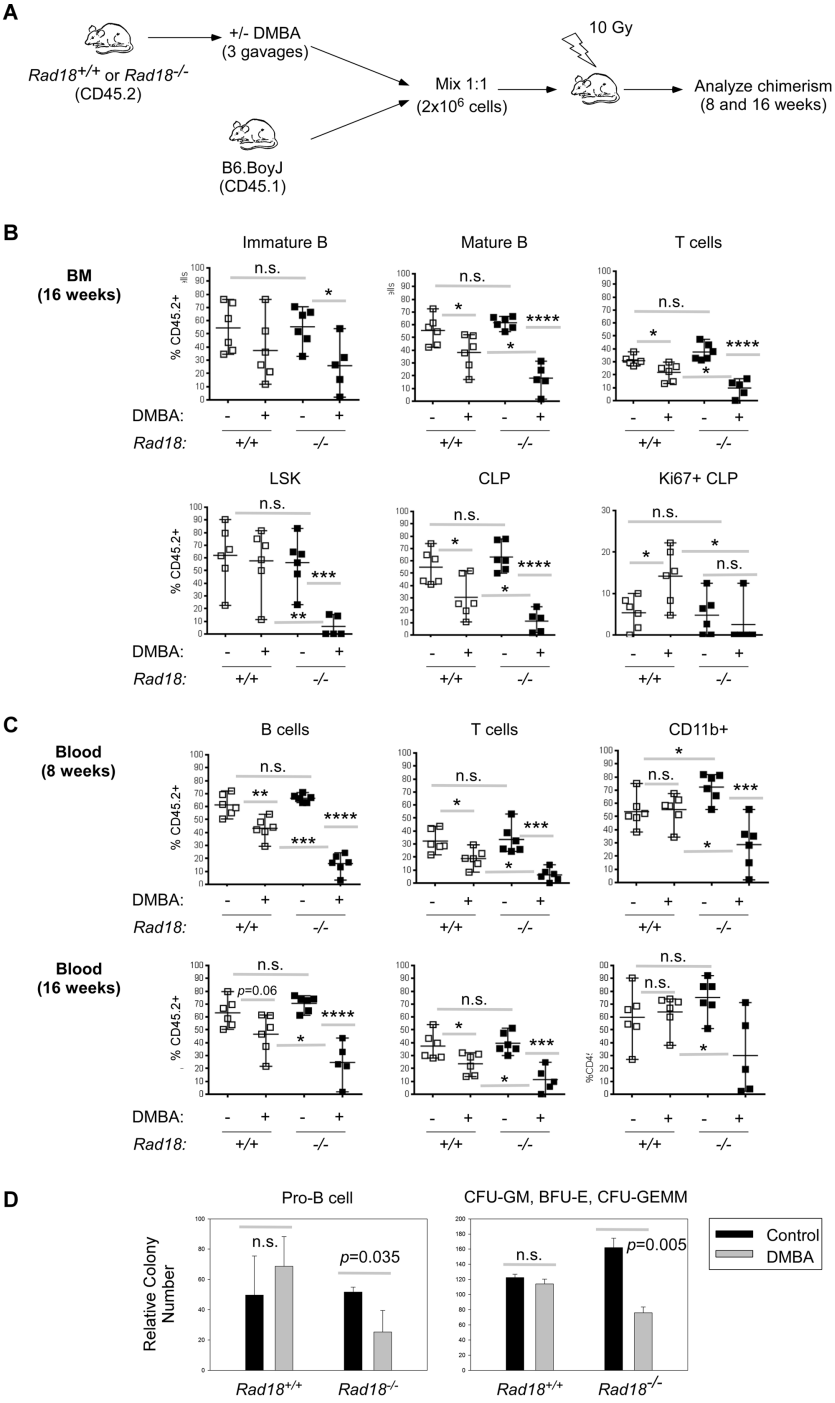

Figure 5. Impaired reconstitution of progenitor and hematopoietic cell populations by *Rad18*$^{-/-}$ HSC from DMBA-treated mice. (**A**) Experimental design for testing effects of repeat DMBA treatments on engraftment potential of *Rad18*$^{+/+}$ and *Rad18*$^{-/-}$ HSC. (**B** and **C**) 8 week-old male *Rad18*$^{+/+}$ and *Rad18*$^{-/-}$ littermate mice were treated with DMBA by oral gavage bi-weekly. Bone marrow cells were harvested 7 days after the third DMBA treatment. Lethally-irradiated WT B6.SJL recipient mice (CD45.1allele) were reconstituted with donor bone marrow from either control or 3X bi-weekly DMBA-treated *Rad18*$^{-/-}$ mice or their WT littermates (each harboring the CD45.2 allele). Prior to transfer, donor bone marrow from each mouse was mixed with competitor bone marrow from normal B6.SJL mice at a 1:1 ratio. At 8 wks (blood) and at 16 wks (blood and bone marrow) following transfer, the frequency of CD45.2 cells in various cell subsets was assessed by flow cytometry (see Supplementary Figure S1 for bone marrow progenitor cell gating strategy). Statistical analysis was performed using an unpaired, two-tailed Student's *t*-test. Mean values significantly different between genotypes are indicated (*$P < 0.05$; **$P < 0.01$; ***$P < 0.001$; ****$P < 0.0001$). (**D**) *Rad18*$^{+/+}$ and *Rad18*$^{-/-}$ littermate mice were treated with DMBA by oral gavage bi-weekly as described for the BM transplant experiment above. Bone marrow cells were harvested 7 days after the third DMBA treatment and cultured in Methocult GF M3434 medium (which supports growth of granulocyte, macrophage–colony-forming units [CFU-GMs]; erythroid–burst-forming units [BFU-Es]; and granulocyte, erythrocyte, macrophage, megakaryocyte–CFUs [CFU-GEMMs]) or MethoCult M3630 (which allows growth of CFU–Pre-Bs) as described under 'Materials and Methods'. Statistical analysis was performed using an unpaired, two-tailed Student's *t*-test. Mean values significantly different between genotypes are indicated (*$P < 0.05$; **$P < 0.01$; ***$P < 0.001$; ****$P < 0.0001$).

bers of mature B-cells T cells and LSK cells derived from transplanted *Rad18*$^{-/-}$ progenitors were reduced by 75% ($P < 0.0001$), 74% ($P < 0.0001$) and 88% ($P < 0.001$), respectively, when the donor mice were DMBA-treated (Figure 5B). Similar results were obtained when we analyzed peripheral blood. For example, 8 weeks following transplant, numbers of *Rad18*$^{+/+}$-progenitor-derived B and T cells were only reduced by 34% ($P < 0.01$) and 44% ($P < 0.05$) when donor mice received DMBA. However, numbers of B and T cells derived from *Rad18*$^{-/-}$ progenitors were reduced by 82% ($P < 0.0001$) and 79% ($P < 0.001$)%, respectively, when the donor mice were administered DMBA (Figure 5C).

We also determined the effects of repeat DMBA treatments on *in vitro* differentiation and proliferative potential of hematopoietic progenitors using colony-forming assays. In BM from DMBA-treated *Rad18*$^{-/-}$ mice there was a 51% decrease in the number of pro-B progenitors ($P = 0.035$) and a 53% decrease in the number of combined erythroid (BFU-E), granulocyte-macrophage (CFU-GM, CFU-M, CFU-G) and multi-potential granulocyte, erythroid, macrophage, megakaryocyte (CFU-GEMM) progenitors ($P = 0.005$) when compared with *Rad18*$^{+/+}$ mice (Figure 5D). In mice that did not receive DMBA, there was no significant difference between *Rad18*$^{+/+}$ and *Rad18*$^{-/-}$ progenitors. Therefore, BM progenitors from DMBA-treated Rad18$^{-/-}$ mice showed reduced *in vitro* colony formation activity when compared with progenitors from *Rad18*$^{+/+}$ littermates (Figure 5D). We conclude that Rad18 is important for hematopoietic progenitors to tolerate long-term PAH genotoxicity.

Effect of Rad18 on PAH-induced hematological malignancy

Reduced DNA damage tolerance of hematopoietic progenitors in BMF syndromes such as FA is associated with genomic instability and increased incidence of hematological malignancy (16,17). Therefore, we determined the effect of Rad18-deficiency on the onset of DMBA-induced hematological malignancies in *Rad18*$^{+/+}$ (n = 26) and *Rad18*$^{-/-}$ (n = 23) mice. Survival rates were indistinguishable between genotypes (Figure 6A). However, post-mortem analysis showed a 1.56-fold increase in the incidence of hematological malignancies in *Rad18*$^{-/-}$ mice compared with *Rad18*$^{+/+}$ animals ($P = 0.05$). Although the difference in incidence of hematological malignancies between genotypes is not significant under the 5% significance level, it is significant under the 10% significance level. Based on the current data, we can say, with high confidence, that the difference between the proportions in the *Rad18*$^{+/+}$ group and the *RAD18*$^{-/-}$ group is around 0.50–0.78 = −0.28. For example, with 95% confidence, it is in the interval (−0.61, 0.04), and with 90% confidence it is in the interval (−0.56, −0.04). We cannot state with certainty in which direction the *P*-value will go if sample size is increased, simply because of random variation. However, based on the current data, if the sample size is increased, it is likely that the difference in proportions will be <0 (the *Rad18*$^{+/+}$ group has a smaller proportion) and the *P*-value will be <0.05.

Staining with appropriate antibodies was used to classify the DMBA-induced hematological malignancies (Figure 6B and Table 1). Interestingly, anti-B220 staining of tu-

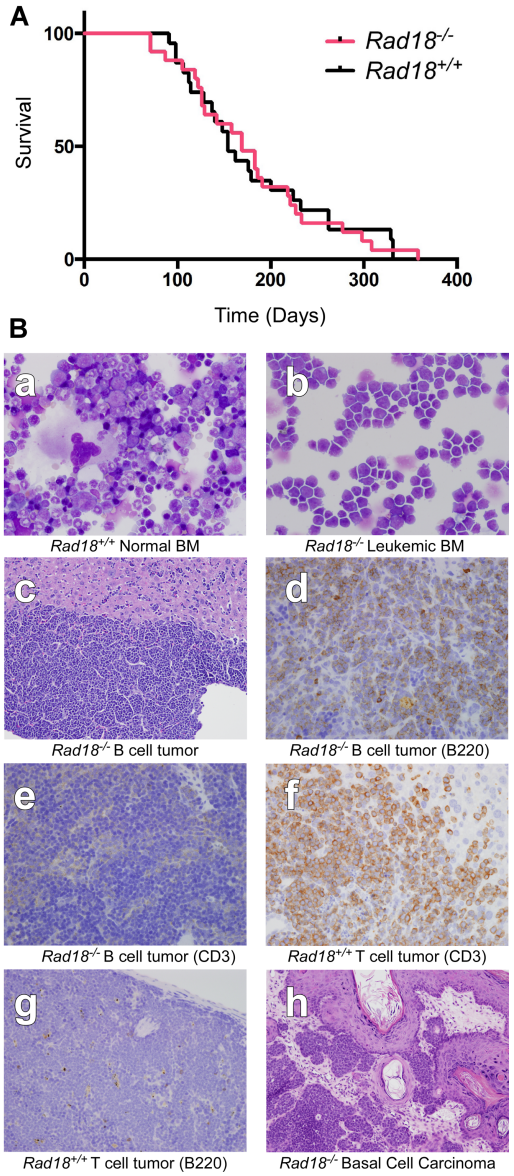

Figure 6. Effects of repeat DMBA treatment on survival and malignancy in *Rad18*$^{+/+}$ and *Rad18*$^{-/-}$ mice. (**A**) Kaplan–Meier plots showing survival rates of *Rad18*$^{+/+}$ and *Rad18*$^{-/-}$ mice after repeat treatment with DMBA. (**B**) Representative DMBA-induced tumors in *Rad18*$^{+/+}$ and *Rad18*$^{-/-}$ mice: (**a**) Wright–Geimsa stained cytospin preparation of a normal bone marrow flush from a *Rad18*$^{+/+}$ mouse (WT7) (original objective magnification 60x) showing maturation of the expected hematopoietic elements including granulocytes, erythroids and megakaryocytes. (**b**) Wright–Geimsa stained cytospin preparation of a bone marrow flush from Rad18$^{-/-}$ mouse (KO9) mice. The expected heterogeneity seen in normal bone marrow (evident in panel (a) is absent. The marrow cells are replaced by a monotonous proliferation of discohesive, large, abnormal lymphoid cells characterized by irregular nuclear contours and scant basophilic cytoplasm. (**c**) Hematoxylin and eosin (H&E) stained sections of liver showing dense infiltrates of large abnormal lymphoid cells (original objective magnification 20x). (**d–g**) B cell and T cell tumors are morphologically indistinguishable. However, immunohistochemical staining identifies B cell tumors (B220-positive/CD3-negative, shown in panels (**d**) and (**e**)) and T cell tumors (CD3-positive/B220-negative, shown in panels (**f**) and (**g**)) (brown chromogen is considered positive with blue counterstain for contrast. original objective magnification 40x). (**h**) Skin lesions from a *Rad18*$^{-/-}$ mouse demonstrating classic features of basal cell carcinoma with nodular collections of hyperchromatic basaloid cells extending from the epidermal surface as indicated by the arrows (original objective magnification 20x).

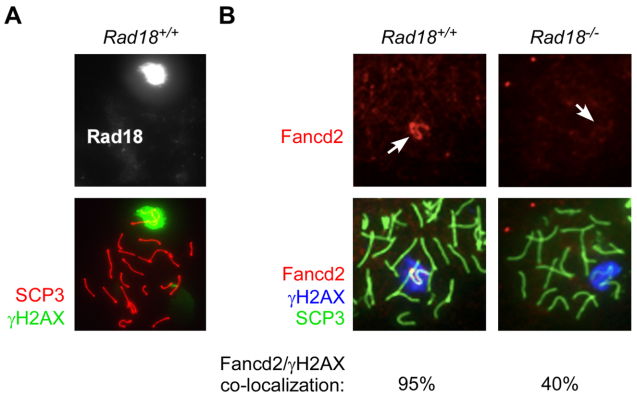

Figure 7. Rad18-dependency of FA pathway activation in meiotic cells. (**A**) Spermatocyte spreads from *Rad18*$^{+/+}$ mice were stained with the indicated antibodies and analyzed by immunofluorescence confocal microscopy. The image shows co-localization of Rad18 (white) with γH2AX (Green) in pachytene spermatocytes from wild-type mice. The synaptonemal complex component SCP3 is shown in Red. Arrowheads indicate positions of the XY chromosomes. (**B**) Spermatocyte spreads from *Rad18*$^{+/+}$ and *Rad18*$^{-/-}$ mice were stained with the indicated antibodies and analyzed by immunofluorescence confocal microscopy. In each of three separate experiments >50 similarly staged meiotic spreads were obtained for each genotype and scored for co-localization of Fancd2 or Fanci with γH2AX. The image shows representative spreads in which there is co-localization of Fancd2 (red) with γH2AX (blue) in pachytene spermatocytes from *Rad18*$^{+/+}$ but not *Rad18*$^{-/-}$ mice. The synaptonemal complex component SCP3 is shown in green. In a Chi square test, the differences in Fancd2 distribution between genotypes were highly significant (*P*-value = 2×10^{-14}).

mor sections revealed a 10-fold increase in the number of B cell-positive malignancies in *Rad18*$^{-/-}$ mice compared to *Rad18*$^{+/+}$ ($P = 0.007$). There was no statistically significant difference in the incidence of T cell-positive malignancies between genotypes.

Rad18-dependent FA pathway activation in germ cells

In addition to its critical roles in ICL repair, the FA pathway mediates DSB processing during normal meiosis. Redistribution of Fancd2 to asynaptic (unpaired) chromosomes in meiotic spermatocytes is a hallmark of FA pathway activation *in vivo* (52). Therefore, we investigated the Rad18-dependency of DSB-induced FA pathway activation in germ cells. Similar to Fancd2, Rad18 was localized to asynaptic meiotic chromosomes, which are readily detectable with intense γH2AX staining (Figure 7A). As expected, Fancd2 co-localized with γH2AX in 95% of the spermatocytes from *Rad18*$^{+/+}$ mice (Figure 7B). However, appropriate redistribution of Fancd2 to asynaptic meiotic chromosomes was reduced to 40% in *Rad18*$^{-/-}$ mice (Figure 7B, upper right panel). Based on Chi square test the difference in Fancd2 localization between genotypes is highly significant ($P = 4 \times 10^{-16}$). Therefore, in contrast with hematopoietic cells (in which Rad18 and Fancd2 are not always co-expressed and Rad18 and FA pathways are independent), FA pathway activation by Spo11-induced DSB is Rad18-dependent in germ cells *in vivo*.

DISCUSSION

Rad18 can promote FA pathway activation (10,12,13) and ICL tolerance in cultured cancer cell lines (11). Specific expression of Rad18 in primary mouse LSK cells and human CD34+ cells (Figure 1A) further compelled the current investigation of potential Rad18 roles in hematopoiesis in a physiological setting. Unexpectedly, we found that untransformed *Rad18*$^{-/-}$ MEF maintain Fancd2 ubiquitination following MMC treatment, yet display hallmarks of FA cells (G2 arrest, MMC-sensitive survival). Why the Rad18-dependency of MMC-induced Fancd2 ubiquitination differs between untransformed MEF and cancer cell lines remains undetermined. Most cancer cells express very high levels of Rad18 protein when compared with primary and untransformed cells. It is possible that FA pathway activation is a 'neomorphic' function resulting from high Rad18 levels. Indeed, ectopic overexpression of Rad18 can promote Fancd2 ubiquitination in the absence of genotoxin treatment (10). Thus although Rad18 may contribute to FA pathway activation in some instances, we demonstrate here that Rad18 is not essential for MMC-induced Fancd2 ubiquitination (Figure 1D–F).

Nevertheless, because *Rad18*$^{-/-}$ MEF are MMC-sensitive, Rad18 might have roles in ICL repair and MMC-tolerance distal to Fancd2 ubiquitination, or via scaffolding of the Smc5/6 complex to ubiquitylated chromatin in the vicinity of damaged chromatin (30). Using MEF from 'knock-in' mice expressing Smc5/6-interaction-deficient RAD18 (Figure 1F), we reveal that scaffolding does not contribute to RAD18-mediated MMC tolerance when RAD18 is present at physiological levels in non-transformed cells. Fancd2 promotes a TLS step during repair of ICL encountered by two converging replication forks (19). Therefore, Rad18-mediated PCNA mono-ubiquitination may facilitate the TLS phase of ICL repair, perhaps explaining why *Rad18*-null MEF are MMC-sensitive despite efficiently mono-ubiquitinating Fancd2 in response to MMC. MMC does induce monoadducts and the MMC-sensitivity of *Rad18*$^{-/-}$ cells could also be explained by reduced TLS activity.

Based on MMC-sensitivity phenotypes of *Rad18*$^{-/-}$ MEF we predicted, but did not find, that *Rad18*$^{-/-}$ mice would exhibit the hallmark hematopoietic defects of *Fanc*-deficient mice (Figure 2). Surprisingly, we found that *Rad18*$^{-/-}$ mice tolerated MMC and displayed no hematopoietic defects (such as reduced hematopoietic progenitor number, reduced HSC proliferative and engraftment potential, MMC-sensitivity or H_2O_2-sensitivity) (Figure 3). Therefore, Rad18 is unlikely to be a core component of the FA pathway in hematopoietic cells. Thus, an important conclusion of this study is that Rad18-dependencies observed in cultured cancer cells are not necessarily representative of Rad18 functions *in vivo*.

Our studies with a carcinogenic PAH (DMBA) (Figure 4), suggest an important *in vivo* role for Rad18 in tolerating certain classes of myelosuppressive agents that affect the Y-family DNA polymerase Polκ. Polκ allows replication of PAH-adducted genomes and prevents DSB and cell death in cultured cells (8,53). Rad18 plays complex roles in the DNA damage response by facilitating replication of dam-

Table 1. Incidence of DMBA-induced hematological malignancies in *Rad18*$^{+/+}$ and *Rad18*$^{-/-}$ mice

	Hematologic malignancies (H&E)	B Cell Lymphoma (B220 positive)	T Cell Lymphoma (CD3 positive)
Rad18$^{+/+}$ (n = 20)	10 (50%)	1 (5%)	6 (30%)
Rad18$^{-/-}$ (n = 23)	18 (78%)	11 (48%)	5 (22%)
P-value	ns	0.007	ns

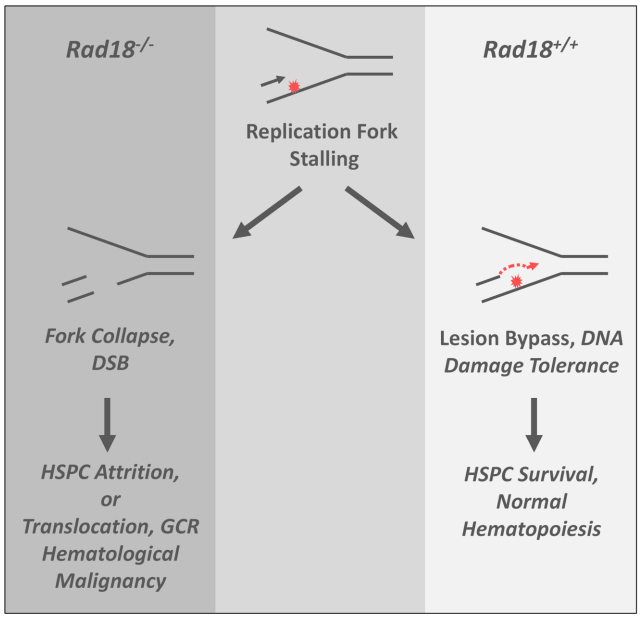

Figure 8. Hypothetical role of Rad18 in HSPC genome maintenance. In wild-type HSPC, Rad18 supports replicative bypass of bulky DNA lesions, conferring DNA damage tolerance and maintaining hematopoiesis in the face of genotoxin exposure. In genotoxin-exposed *Rad18*$^{-/-}$ HSPC, stalled replication forks cannot recover via TLS and collapse leading to DNA DSB formation and attrition of hematopoietic progenitors. Error-prone DSB repair via NHEJ has the potential to generate oncogenic events such as translocations and gross chromosomal rearrangements that drive hematological malignancy.

aged genomes and preventing DNA strand breaks at the expense of replication fidelity. Thus, genome maintenance via Rad18 represents a 'double-edged sword' with the potential to avert genome-destabilizing DSB while causing mutations.

Rad18 has been studied extensively in cell culture systems, yet whether the net effect of Rad18-mediated TLS is tumor-suppressive or oncogenic *in vivo* has not previously been addressed. We show that Rad18-loss can cause a tumor-propensity phenotype at least in the context of B-cell malignancies (Table 1, Figure 6B). Most probably, DSB generated by DMBA-induced fork collapse in Rad18-deficient hematopoietic progenitors initiate oncogenic translocations that drive leukemia (Figure 8). If elevated DSB sustained by early multipotent progenitors accounts for the tumor propensity of *Rad18*$^{-/-}$ mice, it is tempting to speculate that the increased B cell-derived malignancies found involves transcription factors shown to impart skewing toward B-cell acute lymphoid leukemia development (54,55). It is possible that B cell tumorigenesis is unrelated to the viability defect of *Rad18*$^{-/-}$ LSK cells and is related to DMBA-sensitivity of B lineage-committed progenitor cells rather than multipotent progenitors. Alternatively, multipotent progenitors may be the primary targets of DMBA-induced genome instability in *Rad18*$^{-/-}$ mice, potentially conferring 'malignant potential' of all subsequent lineages. However, T cell-committed pre-neoplastic cells may die readily, if they are more dependent on Rad18 for survival compared with B cell lineages: pre-neoplastic cells experience considerable stress during progression to malignancy and B chronic lymphocytic leukemia cells are notoriously resistant to DNA damage (56). Therefore, skewing in favor of B cell malignancies could result if B cell lineages rely less on Rad18 for stress tolerance when compared with other hematopoietic progenitors. It is likely that carcinogen-induced tumorigenesis is driven by error-prone TLS and point mutations in *Rad18*$^{+/+}$ animals but via replication fork collapse, DSB and the ensuing translocations when *Rad18* is absent. Point mutations and translocation-based oncogenic events might predispose to B cell or T cell malignancies, respectively.

Mechanism(s) of FA pathway activation by Rad18 seem to depend on biological context. In response to bulky DNA lesions, the FA pathway is activated secondarily to PCNA mono-ubiquitination (10,13), whereas replication-coupled DSB (in camptothecin-treated cells) trigger RAD18-mediated FA pathway activation independently of PCNA ubiquitination (12). We show that a hallmark of FA pathway activation *in vivo*, namely Fancd2 recruitment to asynaptic chromosomes in spermatocytes is Rad18-dependent (Figure 7). Recruitment of Rad18 to asynaptic chromosomes requires Spo11, the nuclease that generates DSB during meiosis (not shown). Therefore, meiotic regulation of Fancd2 by Rad18 may resemble the Rad18-dependent (PCNA-independent) activation mechanism that occurs in camptothecin-treated cells. *Rad18*$^{-/-}$ and *Fanc*-deficient mice have defective spermatogenesis and fertility defects (15,31,57), possibly related to common defects in meiotic processing of DSB.

In conclusion, we show that the Rad18 and FA pathways are separable *in vivo.* Ours is the first demonstration of a physiological role for Rad18 in DNA damage tolerance, HSC maintenance and suppression of hematological malignancies.

SUPPLEMENTARY DATA

Supplementary Data are available at NAR Online.

ACKNOWLEDGEMENTS

The authors thank Dr Joanne Kurtzberg and Dr Nelson Chao for help obtaining human stem cell products and Dr Jessica Allen for help and advice with flow cytometry. We thank Dr. Robert Weiss for providing Fancd2 and Fanca mutant MEF.

FUNDING

National Institutes of Health (NIH) [R01 HL 129061 to S.S., R21 ES 023895 to C.V. and S.T., and R01 ES09558 to C.V.]. Funding for open access charge: National Institutes of Health [R01 HL 129061 to S.S., R21 ES023895 to C.V. and S.T., and R01 ES09558 to C.V.].
Conflict of interest statement. None declared.

REFERENCES

1. Hanahan,D. and Weinberg,R.A. (2011) Hallmarks of cancer: the next generation. *Cell*, **144**, 646–674.
2. Lehmann,A.R. (2005) Replication of damaged DNA by translesion synthesis in human cells. *FEBS Lett.*, **579**, 873–876.
3. Davies,A.A., Huttner,D., Daigaku,Y., Chen,S. and Ulrich,H.D. (2008) Activation of ubiquitin-dependent DNA damage bypass is mediated by replication protein a. *Mol. Cell*, **29**, 625–636.
4. Tsuji,Y., Watanabe,K., Araki,K., Shinohara,M., Yamagata,Y., Tsurimoto,T., Hanaoka,F., Yamamura,K., Yamaizumi,M. and Tateishi,S. (2008) Recognition of forked and single-stranded DNA structures by human RAD18 complexed with RAD6B protein triggers its recruitment to stalled replication forks. *Genes Cells*, **13**, 343–354.
5. Ulrich,H.D. (2004) How to activate a damage-tolerant polymerase: consequences of PCNA modifications by ubiquitin and SUMO. *Cell Cycle*, **3**, 15–18.
6. Bienko,M., Green,C.M., Crosetto,N., Rudolf,F., Zapart,G., Coull,B., Kannouche,P., Wider,G., Peter,M., Lehmann,A.R. *et al.* (2005) Ubiquitin-binding domains in Y-family polymerases regulate translesion synthesis. *Science*, **310**, 1821–1824.
7. Prakash,S., Johnson,R.E. and Prakash,L. (2005) Eukaryotic translesion synthesis DNA polymerases: specificity of structure and function. *Annu. Rev. Biochem.*, **74**, 317–353.
8. Bi,X., Barkley,L.R., Slater,D.M., Tateishi,S., Yamaizumi,M., Ohmori,H. and Vaziri,C. (2006) Rad18 regulates DNA polymerase kappa and is required for recovery from S-phase checkpoint-mediated arrest. *Mol. Cell. Biol.*, **26**, 3527–3540.
9. Hashimoto,K., Cho,Y., Yang,I.Y., Akagi,J., Ohashi,E., Tateishi,S., de Wind,N., Hanaoka,F., Ohmori,H. and Moriya,M. (2012) The vital role of polymerase zeta and REV1 in mutagenic, but not correct, DNA synthesis across benzo[a]pyrene-dG and recruitment of polymerase zeta by REV1 to replication-stalled site. *J. Biol. Chem.*, **287**, 9613–9622.
10. Song,I.Y., Palle,K., Gurkar,A., Tateishi,S., Kupfer,G.M. and Vaziri,C. (2010) Rad18-mediated translesion synthesis of bulky DNA adducts is coupled to activation of the Fanconi anemia DNA repair pathway. *J. Biol. Chem.*, **285**, 31525–31536.
11. Williams,S.A., Longerich,S., Sung,P., Vaziri,C. and Kupfer,G.M. (2011) The E3 ubiquitin ligase RAD18 regulates ubiquitylation and chromatin loading of FANCD2 and FANCI. *Blood*, **117**, 5078–5087.
12. Palle,K. and Vaziri,C. (2011) Rad18 E3 ubiquitin ligase activity mediates Fanconi anemia pathway activation and cell survival following DNA Topoisomerase 1 inhibition. *Cell Cycle*, **10**, 1625–1638.
13. Geng,L., Huntoon,C.J. and Karnitz,L.M. (2010) RAD18-mediated ubiquitination of PCNA activates the Fanconi anemia DNA repair network. *J. Cell Biol.*, **191**, 249–257.
14. Bargman,G.J., Shahidi,N.T., Gilbert,E.F. and Opitz,J.M. (1977) Studies of malformation syndromes of man XLVII: disappearance of spermatogonia in the Fanconi anemia syndrome. *Eur. J. Pediatr.*, **125**, 163–168.
15. Chen,M., Tomkins,D.J., Auerbach,W., McKerlie,C., Youssoufian,H., Liu,L., Gan,O., Carreau,M., Auerbach,A., Groves,T. *et al.* (1996) Inactivation of Fac in mice produces inducible chromosomal instability and reduced fertility reminiscent of Fanconi anaemia. *Nat. Genet.*, **12**, 448–451.
16. Kee,Y. and D'Andrea,A.D. (2012) Molecular pathogenesis and clinical management of Fanconi anemia. *J. Clin. Investig.*, **122**, 3799–3806.
17. Kee,Y. and D'Andrea,A.D. (2010) Expanded roles of the Fanconi anemia pathway in preserving genomic stability. *Genes Dev.*, **24**, 1680–1694.
18. Kim,H. and D'Andrea,A.D. (2012) Regulation of DNA cross-link repair by the Fanconi anemia/BRCA pathway. *Genes Dev.*, **26**, 1393–1408.
19. Knipscheer,P., Raschle,M., Smogorzewska,A., Enoiu,M., Ho,T.V., Scharer,O.D., Elledge,S.J. and Walter,J.C. (2009) The Fanconi anemia pathway promotes replication-dependent DNA interstrand cross-link repair. *Science*, **326**, 1698–1701.
20. Tebbs,R.S., Hinz,J.M., Yamada,N.A., Wilson,J.B., Salazar,E.P., Thomas,C.B., Jones,I.M., Jones,N.J. and Thompson,L.H. (2005) New insights into the Fanconi anemia pathway from an isogenic FancG hamster CHO mutant. *DNA Repair (Amst)*, **4**, 11–22.
21. Garaycoechea,J.I. and Patel,K.J. (2014) Why does the bone marrow fail in Fanconi anemia? *Blood*, **123**, 26–34.
22. Garaycoechea,J.I., Crossan,G.P., Langevin,F., Daly,M., Arends,M.J. and Patel,K.J. (2012) Genotoxic consequences of endogenous aldehydes on mouse haematopoietic stem cell function. *Nature*, **489**, 571–575.
23. Langevin,F., Crossan,G.P., Rosado,I.V., Arends,M.J. and Patel,K.J. (2011) Fancd2 counteracts the toxic effects of naturally produced aldehydes in mice. *Nature*, **475**, 53–58.
24. Ceccaldi,R., Parmar,K., Mouly,E., Delord,M., Kim,J.M., Regairaz,M., Pla,M., Vasquez,N., Zhang,Q.S., Pondarre,C. *et al.* (2012) Bone marrow failure in Fanconi anemia is triggered by an exacerbated p53/p21 DNA damage response that impairs hematopoietic stem and progenitor cells. *Cell Stem Cell*, **11**, 36–49.
25. Papadopoulo,D., Guillouf,C., Mohrenweiser,H. and Moustacchi,E. (1990) Hypomutability in Fanconi anemia cells is associated with increased deletion frequency at the HPRT locus. *Proc. Natl. Acad. Sci. U.S.A.*, **87**, 8383–8387.
26. Hinz,J.M., Nham,P.B., Salazar,E.P. and Thompson,L.H. (2006) The Fanconi anemia pathway limits the severity of mutagenesis. *DNA Repair (Amst)*, **5**, 875–884.
27. Niedzwiedz,W., Mosedale,G., Johnson,M., Ong,C.Y., Pace,P. and Patel,K.J. (2004) The Fanconi anaemia gene FANCC promotes homologous recombination and error-prone DNA repair. *Mol. Cell*, **15**, 607–620.
28. Nijman,S.M., Huang,T.T., Dirac,A.M., Brummelkamp,T.R., Kerkhoven,R.M., D'Andrea,A.D. and Bernards,R. (2005) The deubiquitinating enzyme USP1 regulates the Fanconi anemia pathway. *Mol. Cell*, **17**, 331–339.
29. Huang,T.T., Nijman,S.M., Mirchandani,K.D., Galardy,P.J., Cohn,M.A., Haas,W., Gygi,S.P., Ploegh,H.L., Bernards,R. and D'Andrea,A.D. (2006) Regulation of monoubiquitinated PCNA by DUB autocleavage. *Nat. Cell Biol.*, **8**, 339–347.
30. Raschle,M., Smeenk,G., Hansen,R.K., Temu,T., Oka,Y., Hein,M.Y., Nagaraj,N., Long,D.T., Walter,J.C., Hofmann,K. *et al.* (2015) DNA repair. Proteomics reveals dynamic assembly of repair complexes during bypass of DNA cross-links. *Science*, **348**, 1253671.
31. Sun,J., Yomogida,K., Sakao,S., Yamamoto,H., Yoshida,K., Watanabe,K., Morita,T., Araki,K., Yamamura,K. and Tateishi,S. (2009) Rad18 is required for long-term maintenance of spermatogenesis in mouse testes. *Mech. Dev.*, **126**, 173–183.
32. Taniwaki,T., Haruna,K., Nakamura,H., Sekimoto,T., Oike,Y., Imaizumi,T., Saito,F., Muta,M., Soejima,Y., Utoh,A. *et al.* (2005) Characterization of an exchangeable gene trap using pU-17 carrying a stop codon-beta geo cassette. *Dev. Growth Differ.*, **47**, 163–172.
33. Rani,R., Li,J. and Pang,Q. (2008) Differential p53 engagement in response to oxidative and oncogenic stresses in Fanconi anemia mice. *Cancer Res.*, **68**, 9693–9702.
34. Peters,A.H., Plug,A.W., van Vugt,M.J. and de Boer,P. (1997) A drying-down technique for the spreading of mammalian meiocytes from the male and female germline. *Chromosome Res.*, **5**, 66–68.
35. Fedoriw,A.M., Menon,D., Kim,Y., Mu,W. and Magnuson,T. (2015) Key mediators of somatic ATR signaling localize to unpaired chromosomes in spermatocytes. *Development*, **142**, 2972–2980.
36. Tateishi,S., Niwa,H., Miyazaki,J., Fujimoto,S., Inoue,H. and Yamaizumi,M. (2003) Enhanced genomic instability and defective postreplication repair in RAD18 knockout mouse embryonic stem cells. *Mol Cell Biol*, **23**, 474–481.
37. Kruyt,F.A., Dijkmans,L.M., Arwert,F. and Joenje,H. (1997) Involvement of the Fanconi's anemia protein FAC in a pathway that signals to the cyclin B/cdc2 kinase. *Cancer Res*, **57**, 2244–2251.
38. Heinrich,M.C., Hoatlin,M.E., Zigler,A.J., Silvey,K.V., Bakke,A.C., Keeble,W.W., Zhi,Y., Reifsteck,C.A., Grompe,M., Brown,M.G. *et al.*

(1998) DNA cross-linker-induced G2/M arrest in group C Fanconi anemia lymphoblasts reflects normal checkpoint function. *Blood*, **91**, 275–287.
39. Carreau,M., Gan,O.I., Liu,L., Doedens,M., Dick,J.E. and Buchwald,M. (1999) Hematopoietic compartment of Fanconi anemia group C null mice contains fewer lineage-negative CD34+ primitive hematopoietic cells and shows reduced reconstruction ability. *Exp. Hematol.*, **27**, 1667–1674.
40. Carreau,M., Gan,O.I., Liu,L., Doedens,M., McKerlie,C., Dick,J.E. and Buchwald,M. (1998) Bone marrow failure in the Fanconi anemia group C mouse model after DNA damage. *Blood*, **91**, 2737–2744.
41. Haneline,L.S., Gobbett,T.A., Ramani,R., Carreau,M., Buchwald,M., Yoder,M.C. and Clapp,D.W. (1999) Loss of FancC function results in decreased hematopoietic stem cell repopulating ability. *Blood*, **94**, 1–8.
42. Barroca,V., Mouthon,M.A., Lewandowski,D., Brunet de la Grange,P., Gauthier,L.R., Pflumio,F., Boussin,F.D., Arwert,F., Riou,L., Allemand,I. *et al.* (2012) Impaired functionality and homing of Fancg-deficient hematopoietic stem cells. *Hum. Mol. Genet.*, **21**, 121–135.
43. Parmar,K., Kim,J., Sykes,S.M., Shimamura,A., Stuckert,P., Zhu,K., Hamilton,A., Deloach,M.K., Kutok,J.L., Akashi,K. *et al.* (2010) Hematopoietic stem cell defects in mice with deficiency of Fancd2 or Usp1. *Stem Cells*, **28**, 1186–1195.
44. N'Jai,A.U., Larsen,M., Shi,L., Jefcoate,C.R. and Czuprynski,C.J. Bone marrow lymphoid and myeloid progenitor cells are suppressed in 7,12-dimethylbenz(a)anthracene (DMBA) treated mice. *Toxicology*, **271**, 27–35.
45. Heidel,S.M., MacWilliams,P.S., Baird,W.M., Dashwood,W.M., Buters,J.T., Gonzalez,F.J., Larsen,M.C., Czuprynski,C.J. and Jefcoate,C.R. (2000) Cytochrome P4501B1 mediates induction of bone marrow cytotoxicity and preleukemia cells in mice treated with 7,12-dimethylbenz[a]anthracene. *Cancer Res.*, **60**, 3454–3460.
46. Page,T.J., O'Brien,S., Jefcoate,C.R. and Czuprynski,C.J. (2002) 7,12-Dimethylbenz[a]anthracene induces apoptosis in murine pre-B cells through a caspase-8-dependent pathway. *Mol. Pharmacol.*, **62**, 313–319.
47. Galvan,N., Jaskula-Sztul,R., MacWilliams,P.S., Czuprynski,C.J. and Jefcoate,C.R. (2003) Bone marrow cytotoxicity of benzo[a]pyrene is dependent on CYP1B1 but is diminished by Ah receptor-mediated induction of CYP1A1 in liver. *Toxicol. Appl. Pharmacol.*, **193**, 84–96.
48. Huggins,C.B. and Grand,L. (1966) Neoplasms evoked in male Sprague-Dawley rat by pulse doses of 7,12-dimethylbenz(a)anthracene. *Cancer Res.*, **26**, 2255–2258.
49. Huggins,C.B. and Sugiyama,T. (1966) Induction of leukemia in rat by pulse doses of 7,12-dimethylbenz(a)anthracene. *Proc. Natl. Acad. Sci. U.S.A.*, **55**, 74–81.
50. Huggins,C.B., Grand,L. and Ueda,N. (1982) Specific induction of erythroleukemia and myelogenous leukemia in Sprague-Dawley rats. *Proc. Natl. Acad. Sci. U.S.A.*, **79**, 5411–5414.
51. Galvan,N., Page,T.J., Czuprynski,C.J. and Jefcoate,C.R. (2006) Benzo(a)pyrene and 7,12-dimethylbenz(a)anthrecene differentially affect bone marrow cells of the lymphoid and myeloid lineages. *Toxicol. Appl. Pharmacol.*, **213**, 105–116.
52. Garcia-Higuera,I., Taniguchi,T., Ganesan,S., Meyn,M.S., Timmers,C., Hejna,J., Grompe,M. and D'Andrea,A.D. (2001) Interaction of the Fanconi anemia proteins and BRCA1 in a common pathway. *Mol. Cell*, **7**, 249–262.
53. Bi,X., Slater,D.M., Ohmori,H. and Vaziri,C. (2005) DNA polymerase kappa is specifically required for recovery from the benzo[a]pyrene-dihydrodiol epoxide (BPDE)-induced S-phase checkpoint. *J. Biol. Chem.*, **280**, 22343–22355.
54. Ungerback,J., Ahsberg,J., Strid,T., Somasundaram,R. and Sigvardsson,M. (2015) Combined heterozygous loss of Ebf1 and Pax5 allows for T-lineage conversion of B cell progenitors. *J. Exp. Med.*, **212**, 1109–1123.
55. Somasundaram,R., Prasad,M.A., Ungerback,J. and Sigvardsson,M. (2015) Transcription factor networks in B-cell differentiation link development to acute lymphoid leukemia. *Blood*, **126**, 144–152.
56. Deriano,L., Guipaud,O., Merle-Beral,H., Binet,J.L., Ricoul,M., Potocki-Veronese,G., Favaudon,V., Maciorowski,Z., Muller,C., Salles,B. *et al.* (2005) Human chronic lymphocytic leukemia B cells can escape DNA damage-induced apoptosis through the nonhomologous end-joining DNA repair pathway. *Blood*, **105**, 4776–4783.
57. Koomen,M., Cheng,N.C., van de Vrugt,H.J., Godthelp,B.C., van der Valk,M.A., Oostra,A.B., Zdzienicka,M.Z., Joenje,H. and Arwert,F. (2002) Reduced fertility and hypersensitivity to mitomycin C characterize Fancg/Xrcc9 null mice. *Hum. Mol. Genet.*, **11**, 273–281.